ELSEVIER

Comparative studies for selective deprotection of the *N*-arylideneamino moiety from heterocyclic amides: kinetic and theoretical studies. Part 2[☆]

Nouria A. Al-Awadi,[*] Yehia A. Ibrahim, Hicham H. Dib, Maher R. Ibrahim,
Boby J. George and Mariam R. Abdallah

Chemistry Department, Kuwait University, PO Box 5969, Safat 13060, Kuwait
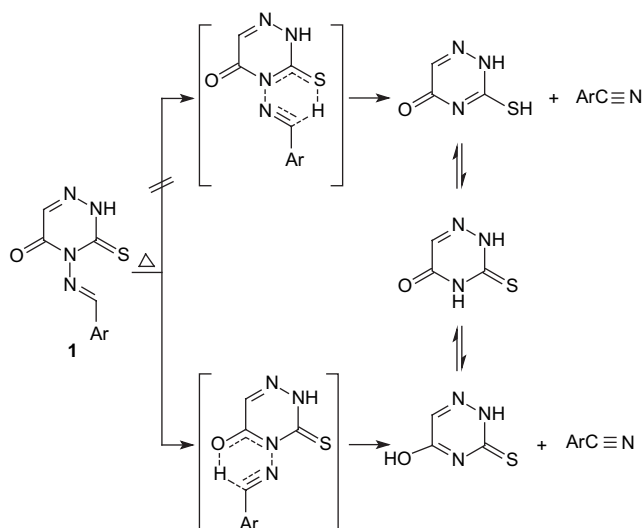
Abstract—4-Benzylideneamino-1,2,4-triazine-3,5(2*H*,4*H*)-diones (**2–5**), 6-styryl-1,2,4-triazine-3,5(2*H*,4*H*)-dione (**6**), and 6-styryl-2,3-di-hydro-3-thioxo-1,2,4-triazin-5(4*H*)-one (**7**) were synthesized and pyrolyzed in the gas phase. The kinetic effect of changing the substituent on the triazine ring from hydrogen to methyl, phenyl, and styryl was measured. Analyses of the pyrolyzates of **2–5** showed the elimination products to be benzonitrile and the triazine fragment, while the pyrolyzates of **6** and **7** reveal the formation of *cis*- and *trans*-cinnamonitriles. Theoretical study of the pyrolysis reactions of **2–5** using an ab initio SCF method was investigated.
© 2006 Elsevier Ltd. All rights reserved.

1. Introduction

Pyrolytic deprotection of 4-arylideneamino-3(2*H*)-thioxo-1,2,4-triazin-5(4*H*)-one (**1**) was carried out.[2] Based on the product analysis together with kinetic results and in the absence of theoretical studies two mechanistic pathways

Scheme 1.

were suggested (Scheme 1). Theoretical studies showed that it is the carbonyl and not the thione bond that attacks the hydrogen atom of the arylideneamino groups.

In this study we have extended the investigation to include 4-benzylideneamino-1,2,4-triazine-3,5-dione derivatives **2–5**, 6-styryl-1,2,4-triazine-3,5(2*H*,4*H*)-dione (**6**), and 6-styryl-2,3-dihydro-3-thioxo-1,2,4-triazin-5(4*H*)-one (**7**).
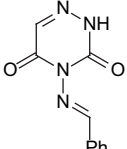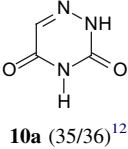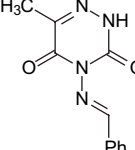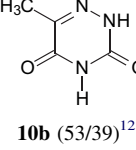
2. Results and discussion
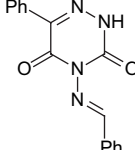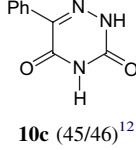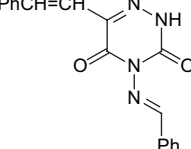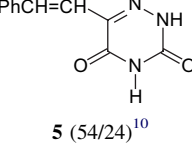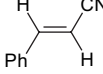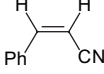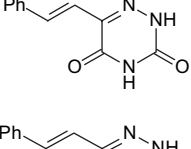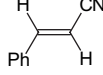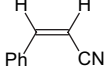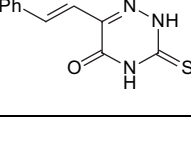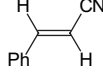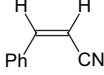
2.1. Product analysis

The substrates **2–7** were prepared and fully characterized by NMR and MS, as described in the Section 3. The products of static as well as flash vacuum pyrolysis of each substrate were analyzed; the constituents of pyrolyzate from **2–5** were ascertained to be benzonitrile[3] together with the heterocyclic fragments **10a**, **10b**, **10c**, and **6** while FVP of **6** and **7** results in *cis*- and *trans*-cinnamonitrile (Table 1).

2.2. Kinetic studies

For each substrate, first-order rate coefficients were obtained at regular temperature intervals. Each rate constant is an average of at least three independent measurements in agreement to within ±2%. The reactions for which the kinetic data were obtained have been ascertained to be homogeneous, unimolecular, non-catalytic, and non-radical processes.[4,5] Arrhenius plots of the data using first-order

Table 1. Pyrolysis products and % yield of compounds **1**–**6** under static/FVP pyrolysis

Compound	Substrate	% Yield (static/FVP)			
		9	**10a–c, 5, 13**	**11**	**12**
1	*(triazine structure)*	Ph—C≡N (42/43)[3]	*(triazine structure)* **10a** (35/36)[12]	—	—
2	H₃C-*(triazine structure)*	Ph—C≡N (32/48)[3]	H₃C-*(triazine structure)* **10b** (53/39)[12]	—	—
3	Ph-*(triazine structure)*	Ph—C≡N (47/28)[3]	Ph-*(triazine structure)* **10c** (45/46)[12]	—	—
4	PhCH=CH-*(triazine structure)*	Ph—C≡N (34/38)[3]	PhCH=CH-*(triazine structure)* **5** (54/24)[10]	Ph—CH=CH—CN **11** (19/13)[17]	Ph—CH=CH—CN **12** (17/10)[17]
5	Ph-CH=CH-*(triazine structure)*	—	—	Ph—CH=CH—CN **11** (18/9)[17]	Ph—CH=CH—CN **12** (14/12)[17]
6	Ph-CH=CH-*(triazine-thione structure)*	—	HS—CN **13**[18]	Ph—CH=CH—CN **11** (38/23)[17]	Ph—CH=CH—CN **12** (25/15)[17]

rate equation: $\log k \,(s^{-1}) = \log A - E_a \,kJ\,mol^{-1}\,(2.303RT)^{-1}$ were strictly linear over ≥95% reaction with correlation coefficient in the range 0.99±0.005. The $\log A$, E_a values and the first-order rate constants of the six compounds under investigation are given in Table 2.

The main features of the kinetic results are as follows:

- Two alternative pathways could be postulated for the extrusion of PhC≡N from **2**–**5**. Pathway (A) involves nucleophilic attack of the C^5=O group on the hydrogen of the arylidene moiety (Scheme 2) while pathway (B) involves the nucleophilic attack of the C^3=O on the same hydrogen atom (Scheme 3). To make the choice between (A) and (B), we have examined both pathways theoretically for compounds **2**–**5**.
- Examination of the free energy of the two suggested pyrolytic pathways of compounds **2**–**5** shows that:
  1. For hydrogen, methyl, phenyl, and styryl substituted compounds (**2**–**5**), the final product P-II can be formed from either pathway **A** or **B** (Fig. 1).

2. With the exception of compound **5**, there is no considerable difference between the TS-I in the two suggested pathways.
3. For each compound, formation of P-I from TS-I requires relatively lower energy via pathway B than that in pathway A. This means that the reaction preferentially involves C^3=O rather than C^5=O in the transition state.

- The overall reactivities of compounds **2**–**5** are the result of electronic synergism involving bonds a, b, and c, and the stabilizing influences associated with the substituents (R) (Scheme 4).
- The reactivity of compound **3** exceeds that of compound **2** by a factor of 1.39×10^4 (Scheme 4), this rate enhancement is attributed to the influence that the methyl substituent has on the delocalization of the lone pair of electrons on N^2 onto the carbonyl oxygen atom of C^3=O group involved in the reaction pathway. This causes an increase in the protophilicity of the bond a, this effect of which the delocalization of this lone pair of electrons on N^2 is exerting is further revealed when

Table 2. Rate coefficients (k/s^{-1}), Arrhenius parameters of compounds **1–6**

Compound	T/K	$10^4 k/s^{-1}$	$\log A/s^{-1}$	$E_a/k\ J\ mol^{-1}$	k_{500K}/s^{-1}
1	548.35	1.455	9.39±0.29	140.58±3.24	7.55×10^{-6}
	588.45	10.66			
	598.35	19.78			
	608.65	28.71			
	618.45	45.88			
2	399.45	0.790	11.35±0.68	119.36±5.44	1.05×10^{-1}
	409.55	1.942			
	419.05	4.582			
	428.85	11.23			
	444.25	26.41			
3	445.45	0.322	12.54±0.07	147.00±0.70	2.31×10^{-3}
	465.35	1.728			
	475.25	3.671			
	485.55	8.146			
	495.65	17.23			
4	456.75	1.332	6.13±0.10	88.572±1.02	9.69×10^{-4}
	471.25	2.643			
	514.55	18.07			
	519.35	20.77			
5	620.95	1.390	6.36±0.07	123.08±0.89	4.66×10^{-7}
	649.75	3.967			
	663.65	6.426			
	677.85	9.750			
	705.95	23.63			
	719.95	35.90			
6	639.85	1.125	6.02±0.33	124.25±4.41	1.56×10^{-7}
	661.55	1.947			
	683.05	3.573			
	704.75	8.391			
	726.45	17.46			
	748.10	29.84			
	770.15	46.17			

(**2**) R = H
(**3**) R = CH$_3$
(**4**) R = C$_6$H$_5$
(**5**) R = PhCH=CH
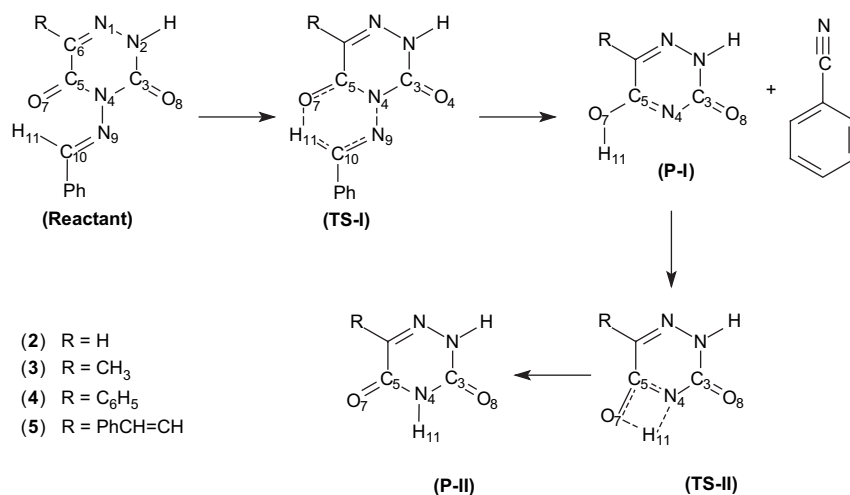
Scheme 2. Pathway A of the suggested mechanism.

the rate of compound **4** is compared with that of compound **3**.
• Changing (R) from methyl in compound **3** to phenyl in compound **4** resulted in reducing the molecular reactivity of compound **4** by a factor of 45.5, this is attributed to the competitive (opposing) delocalization of the lone pair of electrons on N^2 atom of the triazine ring by the phenyl group (Scheme 5).

• This effect explains also:
  (i) The relative reactivity factor of 304.5 of compound **4** over compound **2**.
  (ii) The comparable reactivities of compounds **4** and **5**.
• A reaction mechanism postulated in Scheme 6 is suggested for the formation of *cis*- and *trans*-cinnamonitrile from compounds **6** and **7** together with traces of HSCN from compound **7** (Table 1).
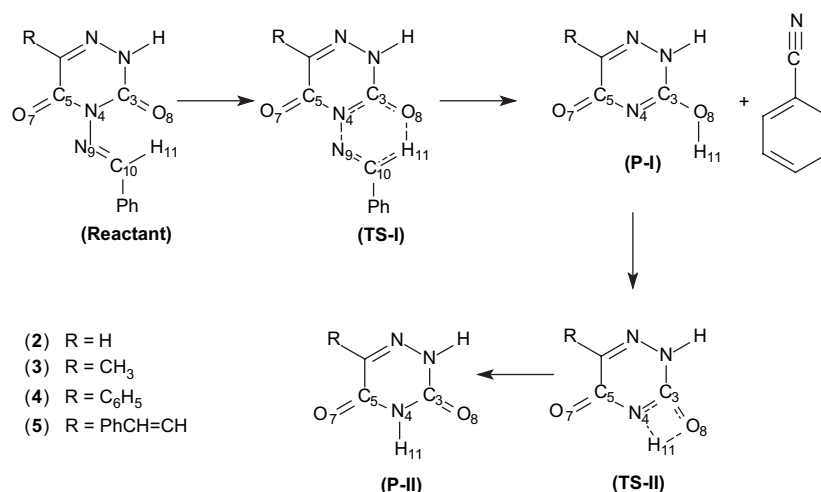
Scheme 3. Pathway B of the suggested mechanism.

(2) R = H
(3) R = CH₃
(4) R = C₆H₅
(5) R = PhCH=CH
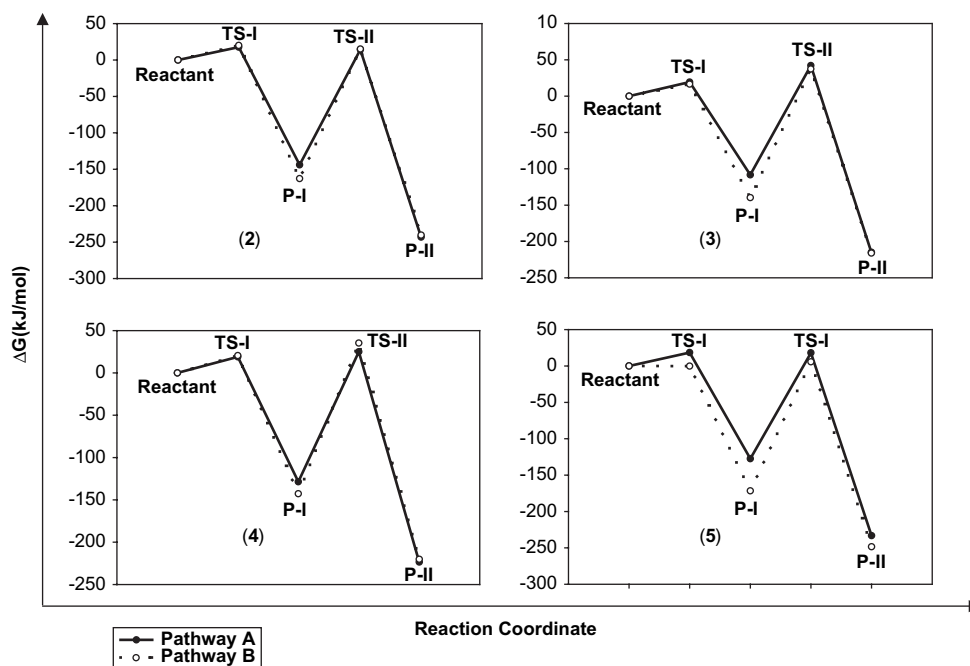
Figure 1. Free energy profile evaluated at the HF/6-31G* level for compounds 2–5.

			k_{rel}
	(3) R = CH₃	(2) R = H	
$k_{500K}/s^{-1}=$	1.05×10^{-1}	7.55×10^{-6}	1.39×10^{4}
	(3) R = CH₃	(4) R = Ph	
$k_{500K}/s^{-1}=$	1.05×10^{-1}	2.30×10^{-3}	45.6
	(4) R = Ph	(2) R = H	
$k_{500K}/s^{-1}=$	2.30×10^{-3}	7.55×10^{-6}	304.6
	(4) R = Ph	(5) R = PhCH=CH	
$k_{500K}/s^{-1}=$	2.30×10^{-3}	9.70×10^{-4}	2.4

Scheme 4. Relative reactivities of compounds 2–5.

This reaction mechanism accounts well for the absence of any electronic effect of changing X from oxygen in 6 to sulfur in 7.

2.3. Computational studies

Ab initio molecular orbital studies on the thermolysis of four-substituted 1,2,4-triazine compounds 2–5, were carried out in the gas phase using SCF method. Calculations were carried out to explore the nature of the reaction mechanism of the unimolecular decomposition of the studied reaction. Two competitive reaction pathways have been studied. Calculations have been performed using TITAN and SPARTAN packages.[6,7]

The geometric parameters of the reactants, the transition states (TS), and the products of the four studied reactions were fully optimized at the HF/6-31G* level to obtain the
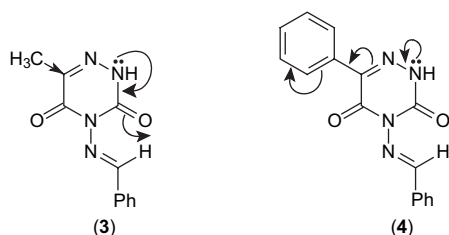
Scheme 5. Opposing delocalization of the lone pair of electrons on N^2 atom by methyl (**3**) and phenyl (**4**) groups.

Scheme 6. Product analyses of compounds **6** and **7**.

energy profiles corresponding to the studied reactions. A scaling factor[8] of 0.9135 for the zero-point vibrational energies has been used. The main distances of the optimized structure of the two pathways of the two studied reactions is represented in Table 3. Electronic energies, zero-point vibrational energies, enthalpies, and entropies, evaluated at the HF/6-31G* level of theory, for all the reactants, transition states, and product involved in the two pathways of the studied reaction are collected in Table 4. The free energy

Table 3. Main distances (Å) of the reactants, TS-I, TS-II, TS-III, TS-IV, P-I, and P-II of the two pathways of the four-substituted compounds, calculated at the HF/6-31G* level

Species	C$_3$–O$_8$	C$_5$–O$_7$	O$_7$–H$_{11}$	C$_{10}$–H$_{11}$	C$_{10}$–N$_9$	N$_4$–H$_{11}$	N$_4$–N$_9$	O$_8$–H$_{11}$
R=H								
Path A								
Reactant	1.188	1.191	2.614	1.079	1.258	2.448	1.401	4.080
TS-I	1.185	1.193	2.080	1.071	1.260	2.617	1.382	4.586
P-I	1.190	1.322	0.948	—	—	3.028	—	5.271
TS-II	1.188	1.249	1.317	—	—	1.323	—	3.041
Path B								
Reactant	1.187	1.190	1.945	1.059	1.258	2.501	1.401	1.945
TS-I	1.195	1.184	2.078	1.071	1.260	2.629	1.382	2.078
P-I	1.316	1.191	0.953	—	—	2.281	—	0.953
TS-II	1.253	1.189	1.308	—	—	1.331	—	1.308
P-II	1.189	1.191	2.481	—	—	1.000	—	2.481
R=CH$_3$								
Path A								
Reactant	1.186	1.193	1.815	1.058	1.257	2.554	1.396	4.594
TS-I	1.186	1.195	2.079	1.071	1.260	2.627	1.382	4.589
P-I	1.191	1.323	0.947	—	—	3.026	—	5.262
TS-II	1.189	1.251	1.316	—	—	1.324	—	3.403
Path B								
Reactant	1.196	1.190	4.605	1.064	1.257	2.525	1.396	1.951
TS-I	1.196	1.185	4.581	1.071	1.259	2.628	1.382	2.072
P-I	1.317	1.193	4.492	—	—	2.279	—	0.953
TS-II	1.254	1.190	3.411	—	—	1.329	—	1.308
P-II	1.192	1.191	2.486	—	—	0.999	—	2.481
R=Phenyl								
Path A								
Reactant	1.181	1.180	1.744	1.038	1.258	2.542	1.403	4.601
TS-I	1.186	1.193	2.086	1.070	1.259	2.647	1.381	4.594
P-I	1.191	1.316	0.954	—	—	2.240	—	5.256
TS-II	1.189	1.253	1.307	—	—	1.321	—	3.390
Path B								
Reactant	1.198	1.187	4.504	1.064	1.258	2.490	1.403	1.909
TS-I	1.196	1.184	4.565	1.071	1.260	2.631	1.383	2.068
P-I	1.317	1.192	4.479	—	—	2.284	—	0.953
TS-II	1.254	1.189	3.386	—	—	1.331	—	1.308
P-II	1.192	1.190	2.455	—	—	1.000	—	2.481
R=PhCH=CH								
Path A								
Reactant	1.189	1.192	2.717	1.079	1.257	2.433	1.401	3.944
TS-I	1.186	1.194	2.097	1.071	1.259	2.654	1.381	4.595
P-I	1.191	1.320	0.949	—	—	3.013	—	4.492
TS-II	1.189	1.254	1.309	—	—	1.323	—	4.348
Path B								
Reactant	1.194	1.187	4.094	1.078	1.258	2.460	1.401	2.575
TS-I	1.196	1.185	4.569	1.070	1.260	2.627	1.384	2.058
P-I	1.313	1.198	4.457	—	—	2.276	—	0.954
TS-II	1.255	1.191	3.378	—	—	1.329	—	1.309
P-II	1.193	1.191	2.448	—	—	1.000	—	2.481

Table 4. Total energy, zero-point vibrational energy (ZPE) and thermal correction to enthalpy and entropy at HF/6-31G* for the two pathways of the four studied reactions

Species	Total energy (Hartree)	ZPE (kcal/mol)	Enthalpy (kcal/mol)	Entropy
R=H				
Pathway A				
R	−750.818948	120.113	127.63	111.907
TS-I	−750.816035	120.036	127.075	107.121
P-I	−428.390523	50.859	54.482	77.457
TS-II	−428.326590	47.769	51.182	76.326
Pathway B				
R	−750.819075	120.124	127.677	112.895
TS-I	−750.816123	120.011	127.06	107.211
P-I	−428.398918	51.036	54.652	77.529
TS-II	−428.327099	47.767	51.215	76.584
P-II	−428.428879	51.339	54.934	77.531
R=CH₃				
Pathway A				
R	−789.847659	138.917	146.924	114.956
TS-I	−789.859391	138.634	146.654	114.164
P-I	−467.432060	69.519	74.072	84.270
TS-II	−467.370078	66.306	70.756	84.052
Pathway B				
R	−789.847626	138.807	146.823	115.701
TS-I	−789.859867	138.607	146.644	114.384
P-I	−467.443538	69.632	74.203	84.584
TS-II	−467.371790	66.363	70.777	83.687
P-II	−467.472906	69.945	74.518	84.785
R=Phenyl				
Pathway A				
R	−980.323127	174.213	182.91	119.782
TS-I	−980.366412	174.408	184.171	129.535
P-I	−657.944562	105.496	111.736	100.159
TS-II	−657.880994	102.288	108.418	108.443
Pathway B				
R	−980.360354	174.604	184.363	130.6
TS-I	−980.366976	174.413	184.187	129.724
P-I	−657.950982	105.494	111.774	100.546
TS-II	−657.879006	102.236	108.357	99.479
P-II	−657.980931	105.843	112.109	100.544
R=PhCH=CH				
Pathway A				
R	−1057.258752	197.233	208.812	145.891
TS-I	−1057.25448	197.072	208.199	141.538
P-I	−734.828937	128.141	135.741	112.727
TS-II	−734.769220	124.933	132.416	112.019
Pathway B				
R	−1057.258991	197.102	207.682	136.564
TS-I	−1057.25538	197.093	208.241	142.02
P-I	−734.839730	128.205	135.847	113.125
TS-II	−734.767977	124.949	132.443	112.211
P-II	−734.869487	128.550	136.184	113.414

profile for the decomposition process of the two studied reactions is presented in Figure 1.

Examination of the free energy of the two suggested pathways of the four-substituted reactions studied shows that, for hydrogen, methyl, and phenyl substituted compounds the final product can be formed from either of the two pathways, since there is no large differences between the transition state one (TS-I) in the two pathways. Just in styryl, it appears clearly the formation for the final product (P-II) is favored via pathway B than pathway A, since the six-membered cyclic transition state (TS-I) is of lower energy in pathway A than in pathway B. The calculated activation energies of TS-I are 18.40 and −0.25 kJ/mol for the reaction via pathway A and pathway B, respectively. Although the formation of P-I is more favored for pathway B than

pathway A. The difference between the activation energies of P-I in the two pathways is 44.18 kJ/mol.

3. Experimental

3.1. Synthesis

All melting points are uncorrected. IR spectra were recorded in KBr disk using Perkin–Elmer system 2000 FTIR spectrophotometer. ¹H NMR spectra were recorded on a BRUKER DPX 400 MHz Superconducting NMR spectrometer. Mass spectra were measured on Vg Auto-spes-q (high resolution, high performance, tri-sector GC/MS/MS) and with LCMS using Agilent 1100 series LC/MSD with an API-ES/APCI ionization mode. Microanalyses were performed on LECO CHNS-932 Elemental Analyzer.

3.1.1. 4-Benzylidineamino-1,2,4-triazine-3,5(2*H*,4*H*)-diones (2–5).

3.1.1.1. General procedure. A mixture of the appropriate 4-amino-1,2,4-triazine derivatives (5 mmol)[9] in acetic acid (10 mL) together with benzaldehyde (0.5 g, 5 mmol) and anhydrous sodium acetate (500 mg) was heated under reflux for 2 h. The solid that precipitated after cooling was collected and recrystallized from ethanol.

3.1.1.2. 4-Benzylidineamino-1,2,4-triazine-3,5(2*H*,4*H*)-dione (2). Colorless crystals from ethanol, yield 800 mg (74%), mp 205–207 °C. LCMS *m/z*=217 (M+1). IR: 3221, 3111, 3052, 2941, 1714, 1665, 1612, 1570, 1401, 1341, 1230, 1097, 976, 833, 743. ^{1}H NMR (CDCl$_3$) δ 9.75 (br, 1H, NH), 8.68 (s, 1H), 7.92 (d, 2H, *J* 8), 7.60 (m, 1H), 7.54 (s, 1H), 7.48 (t, 2H, *J* 7.6). ^{13}C NMR (DMSO) δ 172.6, 154.2, 148.1, 136.3, 134.1, 132.9, 130.2, 129.9. Anal. Calcd for C$_{10}$H$_8$N$_4$O$_2$ (216.2): C, 55.56; H, 3.73; N, 25.91. Found: C, 55.56; H, 3.67; N, 25.87.

3.1.1.3. 4-Benzylidineamino-6-methyl-1,2,4-triazine-3,5(2*H*,4*H*)-dione (3). Colorless crystals from ethanol, yield 900 mg (78%), mp 190–192 °C. LCMS *m/z*=231 (M+1). IR: 3252, 3189, 2927, 1733, 1684, 1660, 1615, 1423, 1373, 1280, 1239, 795, 760, 690. ^{1}H NMR (CDCl$_3$) δ 9.73 (br, 1H, NH), 8.66 (s, 1H), 7.91 (dd, 2H, *J* 8, 1.4), 7.56 (m, 1H), 7.44 (m, 2H), 2.31 (s, 3H). ^{13}C NMR (CDCl$_3$) δ 169.9, 153.8, 148.1, 144.5, 133.4, 132.1, 129.7, 129.2, 17.3. Anal. Calcd for C$_{11}$H$_{10}$N$_4$O$_2$ (230.2): C, 57.39; H, 4.38; N, 24.34. Found: C, 57.35; H, 4.40; N, 24.38.

3.1.1.4. 4-Benzylidineamino-6-phenyl-1,2,4-triazine-3,5(2*H*,4*H*)-dione (4). Colorless crystals from ethanol, yield 1.20 g (82%), mp 230–232 °C. LCMS *m/z*=293 (M+1). IR: 3224, 3140, 3118, 3033, 2935, 1731, 1683, 1659, 1446, 1415, 1298, 1247, 1167, 768, 685. ^{1}H NMR (CDCl$_3$) δ 9.77 (br, 1H, NH), 8.70 (s, 1H), 7.99 (dd, 2H, *J* 8, 1.4), 7.94 (d, 2H, *J* 8.0), 7.57 (m, 1H), 7.53–7.45 (m, 5H). ^{13}C NMR (DMSO) δ 173.0, 153.8, 148.0, 142.4, 134.1, 133.7, 133.0, 130.6, 130.2, 129.9, 129.2, 129.0. Anal. Calcd for C$_{16}$H$_{12}$N$_4$O$_2$ (292.3): C, 65.75; H, 4.14; N, 19.17. Found: C, 65.55; H, 3.96; N, 19.10.

3.1.1.5. 4-Benzylidineamino-6-styryl-1,2,4-triazine-3,5(2*H*,4*H*)-dione (5). Colorless crystals from ethanol, yield 1.30 g (82%), mp 260–262 °C. LCMS *m/z*=319 (M+1). IR: 3322, 3236, 3081, 2945, 1723, 1653, 1562, 1418, 1317, 1199, 972, 941, 741. ^{1}H NMR (DMSO-d_6) δ 12.90 (br, 1H, NH), 8.79 (s, 1H), 7.92 (d, 2H, *J* 7.6), 7.74 (d, 1H, *J* 16.4), 7.67–7.57 (m, 5H), 7.43–7.33 (m, 3H), 7.14 (d, 1H, *J* 16.4). ^{13}C NMR (DMSO) δ 173.0, 153.9, 147.8, 140.9, 137.0, 135.0, 134.1, 133.0, 130.2, 130.0, 129.9, 129.1, 128.2, 121.0. Anal. Calcd for C$_{18}$H$_{14}$N$_4$O$_2$ (318.3): C, 67.92; H, 4.43; N, 17.60. Found: C, 67.88; H, 4.41; N, 17.58.

3.1.1.6. 6-Styryl-1,2,4-triazine-3,5(2*H*,4*H*)-dione (6). Prepared as reported,[10] mp 268–270 °C (lit.[9] 266 °C). ^{1}H NMR (DMSO-d_6) δ 12.41 (br, 1H, NH), 12.09 (br, 1H, NH), 7.69 (d, 1H, *J* 16.4), 7.60 (d, 2H, *J* 7.4), 7.39 (t, 2H, *J* 7.4), 7.33 (m, 1H), 7.05 (d, 1H, *J* 16.4).

3.1.1.7. 6-Styryl-2,3-dihydro-3-thioxo-1,2,4-triazine-5(4*H*)-one (7). Prepared as reported,[10] mp 278–280 °C

(lit.[11] 264 °C). ^{1}H NMR (DMSO-d_6) δ 12.63 (br, 1H, NH), 12.23 (br, 1H, NH), 7.79 (d, 1H, *J* 16.4), 7.64 (d, 2H, *J* 7.4), 7.42–7.33 (m, 3H), 7.07 (d, 1H, *J* 16.4).

3.1.1.8. 1,2,4-Triazine-3,5(2*H*,4*H*)-dione (10a). Mp 282–283 °C (lit.[12] 283 °C). ^{1}H NMR (DMSO-d_6) δ 12.32 (br, 1H, NH), 11.96 (br, 1H, NH), 7.38 (s, 1H).

3.1.1.9. 6-Methyl-1,2,4-triazine-3,5(2*H*,4*H*)-dione (10b). Mp 215–216 °C (lit.[12] 216 °C). ^{1}H NMR (DMSO-d_6) δ 11.99 (br, 1H, NH), 11.88 (br, 1H, NH), 2.50 (s, 3H, CH$_3$).

3.1.1.10. 6-Phenyl-1,2,4-triazine-3,5(2*H*,4*H*)-dione (10c). Mp 262–263 °C (lit.[12] 262 °C). ^{1}H NMR (DMSO-d_6) δ 12.52 (br, 1H, NH), 12.11 (br, 1H, NH), 7.82 (d, 2H, *J* 7.4, Ar–H), 7.43 (m, 3H, Ar–H).

3.2. Pyrolysis

3.2.1. Static pyrolysis. Each of the substrates **2–7** (200 mg) was introduced into the reaction tube (1.5×12 cm Pyrex), cooled in liquid nitrogen, sealed under vacuum (0.06 mbar) and then placed in the pyrolyzer for 15 min at a temperature deemed necessary for complete pyrolysis of the substrate. The pyrolyzate was then separated by preparative HPLC using ABZ$^+$ column and an eluent of suitable composition (acetonitrile and water). The collected solutions of the pyrolyzate fractions were evaporated and each fraction was subjected to ^{1}H NMR, GC–MS, and LC–MS analyses (Table 1).

3.2.2. Flash vacuum pyrolysis (FVP). The apparatus used was similar to the one, which has been described in our recent publications.[5,13] The sample was volatilized from a tube in a Büchi Kugelrohr oven through a 30×2.5 cm horizontal fused quartz tube. This was heated externally by a Carbolite Eurotherm tube furnace MTF-12/38A to a temperature of 600 °C, the temperature being monitored by a Pt/Pt–13%Rh thermocouple situated at the center of the furnace. The products were collected in a U-shaped trap cooled in liquid nitrogen. The whole system was maintained at a pressure of 10^{-2} Torr by an Edwards Model E2M5 high-capacity rotary oil pump, the pressure being measured by a Pirani gauge situated between the cold trap and the pump. Under these conditions the contact time in the hot zone was estimated to be ≅10 ms. The different zones of the products collected in the U-shaped trap were analyzed by ^{1}H NMR, LC–MS, and GC–MS. Relative and percent yields were determined from ^{1}H NMR. Identities of compounds obtained were confirmed by comparison of their ^{1}H NMR with data of products separated from preparative HPLC (Table 1).

3.3. Kinetic runs and data analyses

A stock solution (7 mL) was prepared by dissolving 6–10 mg of the substrate in acetonitrile as solvent to give a concentration of 1000–2000 ppm. An internal standard was then added, the amount of which was adjusted to give the desired peak area ratio of substrate to standard (2.5:1). The solvent and the internal standard are selected because both are stable under the conditions of pyrolysis, and because they do not react with either substrate or product. The internal standard used in this study is chlorobenzene, 1,3-dichlorobenzene or 1,2,4-trichlorobenzene. Each solution was filtered to ensure

that a homogeneous solution is obtained. The weight ratio of the substrate with respect to the internal standard was calculated from the ratio of the substrate peak area to the peak area of the internal standard. The kinetic rate was obtained by tracing the rate of disappearance of the substrate with respect to the internal standard as follows: an aliquot part (0.2 mL) of each solution containing the substrate and the internal standard is pipetted into the reaction tube, which is then placed in the pyrolyzer for 6 min under non-thermal conditions. A sample is then analyzed using a Waters HPLC probe (pump model 515, UV detector model 2487), or a Metrohm HPLC (pump model 7091C, and SPD 10 AV Shimadzo UV detector) and UV detector at wavelength of 256 nm, and the standardization value (A_0) was then calculated. Several HPLC measurements were obtained with an accuracy of $\geq 2\%$. HPLC columns used for the analysis were Supelco (25 cm length, 4.6 mm ID) ABZ$^+$, LC-8, and LC-18. The temperature of the pyrolysis (aluminum) block is then raised and held for ca. 900 s to allow approximately 10% pyrolysis to take place at this temperature. This procedure is repeated after each 10–15 °C rise in the temperature of the pyrolyzer until $\geq 90\%$ pyrolysis takes place. The relative ratios of the integration values of the sample and the internal standard (A) at the pyrolysis temperature are then calculated. A minimum of three kinetic runs were carried out at each reaction temperature, following every 10–15 °C rise in the temperature of the pyrolyzer, in order to ensure reproducible values of (A). Treatment of the kinetic data has been detailed elsewhere.[14–16]

Acknowledgements

References and notes

1. Part 1: George, B. J.; Dib, H. H.; Abdallah, M. R.; Ibrahim, M. R.; Khalil, N. S.; Ibrahim, Y. A.; Al-Awadi, N. A. *Tetrahedron* **2006**, *62*, 1182–1192.
2. Al-Etaibi, A.; Abdallah, M. R.; Al-Awadi, N.; Ibrahim, Y.; Hasan, M. *J. Phys. Org. Chem.* **2004**, *17*, 49–55.
3. *FT-NMR Aldrich Catalog 1(2)*; Milwaukee: Wisconsin, USA, 1509A.
4. Al-Awadi, N. A.; Elnagdi, M. H.; Mathew, T. *Int. J. Chem. Kinet.* **1995**, *27*, 517–523.
5. Al-Awadi, N.; Kaul, K.; El-Dusouqui, O. M. E. *J. Phys. Org. Chem.* **2000**, *13*, 499–504.
6. *Titan*; Wavefunction: Irvine, USA, 1999.
7. *Spartan '04 for Windows*; Wavefunction: USA, 2004.
8. Scott, A.; Radom, L. *J. Phys. Chem.* **1996**, *100*, 16502–16513.
9. Ibrahim, Y. A.; Eid, M. A.; Badawy, M. A.; Abdel-Hady, S. A. *J. Heterocycl. Chem.* **1981**, *18*, 953–956.
10. Ibrahim, Y. A.; Eid, M. A. *Indian J. Chem.* **1975**, *13*, 1098–1100.
11. Semonsky, M., et al. *Collect. Czech. Chem. Commun.* **1967**, *12*, 4439–4451.
12. Lalezari, I. *J. Org. Chem.* **1968**, *33*, 4281–4283.
13. Ibrahim, Y. A.; Al-Awadi, N. A.; Ibrahim, M. R. *Tetrahedron* **2004**, *60*, 9121–9130.
14. Sharp, J. T.; Gosney, I.; Rowley, A. G. *Practical Organic Chemistry*; Chapman & Hall: London, 1989; p 51.
15. Al-Awadi, N. A.; Elnagdi, M. H.; Kaul, K.; Ilingovan, S.; El-Dusouqui, O. M. E. *J. Phys. Org. Chem.* **1999**, *12*, 654–656.
16. Al-Awadi, N. A.; El-Dusouqui, O. M. E.; Kaul, K.; Dib, H. H. *Int. J. Chem. Kinet.* **2000**, *32*, 403–407.
17. Huang, X.; Xie, H.; Wu, H. *J. Org. Chem.* **1988**, *53*, 4862–4864.
18. HSCN was detected by its MS correct parent ion peak (M$^+$,59) in comparison with authentic sample prepared by treating KSCN and Dowex-50w.